IIETA International Information and Engineering Technology Association
Advancing the World of Information and Engineering

Instrumentation Mesure Métrologie
Vol. 24, No. 3, June, 2025, pp. 229-236
Journal homepage: http://iieta.org/journals/i2m

Preparation of New Azo Dye Derived of Pharmaceutical Substances (Procaine and Vitamin B6) and Theoretically Studied as a Carbon Steel Corrosion Inhibitor

Hasanain A. Abdullmajed[1*], Ihsan A. Alasady[1], Hadi T. Obaid[2], Ghufran A. Mirdan[3], Nuha A. M. Obaid[1]

[1] Department of Chemistry, College of Education for Pure Sciences, University of Basrah, Basrah 61007, Iraq
[2] Department of English, College of Education, Al-Shatrah University, Thi-Qar 64002, Iraq
[3] General Directorate of Education in Basrah, Ministry of Education, Basrah 61007, Iraq

Corresponding Author Email: hasanain.abdullmajed@uobasrah.edu.iq

https://doi.org/10.18280/i2m.240304

Received: 16 September 2024
Revised: 12 April 2025
Accepted: 20 June 2025
Available online: 30 June 2025

Keywords:
procaine, vitamin B6, azo dyes, acid-base properties, isopiestic-p, point, solvent effect, corrosion inhibitor, theoretical study, computational chemistry

ABSTRACT

The amine drug procaine hydrochloride is employed in the preparation of the current azo dye, added to another drug, pyridoxine hydrochloride 2-(diethylamino) ethyl (Z)-4-(5-hydroxyl-3,4-bis(hydroxymethyl)-6-methylpyridin-2-yl) benzoate. Chemical diagnosis of the prepared chemical compound was done using infrared technology, and mass spectrometry electron spectra were performed for the prepared compound in terms of its basic and acidic properties, which includes determining the protonation constant and the ionization constant at different pH values (2-12), as well as knowing the number of apparent isopiestic points. To the altar of mindful clarification to achieve the highest moisture of azo dye L (pH 12), several clarifying agents were prepared that gave a pH of 12. The theoretical study results also indicated that the new dye (L2) is not as effective at preventing corrosion in carbon steel as the original azo dye (L1) it comes from. Therefore, it is assumed from the above that the experimental results, if conducted, would need to demonstrate a corrosion inhibition efficiency of the inhibitor (L2) that exceeds the value of the inhibitor inhibition efficiency (L1), as predicted by the theoretical results in the computational chemistry program.

1. INTRODUCTION

Azo dyes are among the most significant types of organic dyes in pharmaceutical drugs. It has many uses in many practical applications such as analytical chemistry, the textile industry, dyeing, food, cosmetics, and pharmaceuticals [1, 2]. Because it has biological activities and chemical and physical properties, these compounds are used in more pharmaceutical ablate and agreed for their application as anti-neoplastic, anti-diabetics, anti-septic, anti-fungal, anti-bacterial, and anti-inflammatory infections [3-6]. They have a lot of gains more than the other most typical combination, bright, strong colors that are stable throughout the pH lineup, heat-stable, and unaffected by light or air. Azo-dyes can be thought about as N-donor ligands and occupy a broad area of research [7]. Metal complexes of azo dyes have received a lot of attention recently because of their potential applications in catalytic processes that can have a large industrial dimension [8]. The vitamin B6 group contains a pyridine ring in its molecule, the group of six members: pyridoxamine-5-phosphate, pyridoxine, pyridoxamine, pyridoxal, pyridoxal-5-phosphate and, pyridoxine-5-phosphate [9]. The pyridoxine hydrochloride [pyridoxol hydrochloride, 5-hydroxy-6-methylpyridine-3,4-diyl) methanol hydrochloride] was determined in pharmaceutical substances spectrophotometrically as an azo dye with 2,4-dinitrophenylhydrazine of the red color of max. Wavelength (522 nm) [10], beer's law up to (12.5 µg.ml^{-1}) and molar absorption coefficient (15214 l.mol^{-1}.cm^{-1}). It was also used to determine in pharmaceutical substances spectrophotometrically as an azo dye with 4-nitroaniline at max. wavelength (480 nm) [11], beer's law in the range of (5-500 µg.ml^{-1}) and molar absorption coefficient (27000 l.mol^{-1} .cm^{-1}). And used as azo dye with the drug ethyl-4-amino benzoate. Azo dye has also been used to resolve the nitrite response to [12]. The procaine hydrochloride 2-(diethylamino) ethyl-4-aminobenzoate hydrochloride] is a good aromatic amine drug for forming azo dyes, for example with acetylacetone. The dye forms with copper and nickel (1:2) molar ratios complexes [13]. Procaine hydrochloride also azo dyes with imidazole, phenylephrine, oxindol, and 4,5-diphenyl imidazole [14]. Procaine hydrochloride forms a new azo dye with 4-amino antipyrine [15] at the max wavelength (360 nm). The basic and acidic properties were studied at different pH values (2-12), and then the protonation and ionization constants were calculated, as well as the effect of solvents chemicals for the more polarities of as prepared compounds. The interaction for aromatic amine procaine hydrochloride with salicylic acid [16]. Many applications have been made to this dye such as strong acid and strong base as well as nitrite determination, acid-base properties, and the solvent effect of different polarities were studied. The present work includes the preparation of a new azo dye derived from procaine and vitamin B6 (L). The electronic spectra of the compound prepared in this research were diagnosed in terms of basic and

acidic properties, identification of protons, calculating ionization constants, and studying the effect of solvents with different polarities. The study showed that the prepared dye is an excellent, inexpensive, and easy-to-prepare corrosion inhibitor, which can be used to dispense with expensive corrosion inhibitors.

2. EXPERIMENTAL

All chemicals used in the preparation were of very high purity and deionized and solvent-free distilled water (for spectroscopic use) was used. Reaction conditions: The dye was prepared at a temperature of 5 to 0 degrees Celsius, and the dye was adjusted in a neutral medium and also re-purified using ethanol and hexane solvent.

2.1 Materials and synthesis

Infrared spectra were noted as potassium bromide discs using a JASCO/Japan FT-IR 4200. Melting points warmth scientific [9100]. Visible spectra tracked by JENWAY [6305] Spectrophotometer. Mass spectra were stated by the EI technique deploying Agilent Technologies in one device. pH values were calculated using a pH meter from [Oakion pH 2100 Series] and an accurate balance. The azo dye reagent (L) was prepared by the recommended method [17] by coupling 0.06 mole of diazonium salt of procaine hydrochloride with an alkaline solution of 0.06 mole of pyridoxine hydrochloride at 0℃. The prepared dye is neutralized by adding a dilute solution of hydrochloric acid to it and making the environment slightly acidic to convert the azo dye from the sodium salt formula to the hydrogen formula, and the pH is adjusted between 6 and 7. The precipitate formed in a Büchner funnel was filtered, dried, recrystallized using ethyl alcohol, and its melting point measured. The chemical composition of the prepared azo dye was proposed as in Scheme 1.

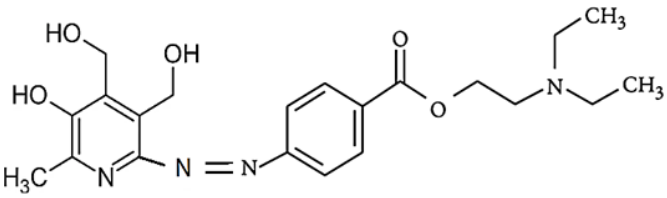

Scheme 1. Azo dye L. L: 2-(diethylamino) ethyl Z-4-[(5-hydroxyl-3,4-bis(hydroxymethyl)-6-methylpyridin-2-yl] benzoate

2.2 The solutions used

- (1×10^{-3} M) orange ethanolic stock azo dye.
- Universal and solution (pH 2-12) [18].
- Different kinds of buffer solutions of (pH 12) [18].

2.3 Effect of solvents on the visible absorption spectra of the prepared dye

A series of solutions of L of overall quantities (8×10^{-5} M) was completed in n-hexane, benzene, 1,4-dioxane, diethyl ether, chloroform, ethyl acetate, THF, dichloromethane, n-hexane, acetone, ethanol, and DMSO. The solvent was used as a reference solution, and then the absorbance was recorded for all the prepared solutions in a range of wavelengths (340-540 nm).

2.4 Visible absorption spectrum of the dye in solutions of different pH values

A series of protective solutions with different values of pH (2-12) with a total azo dye L concentration (8×10^{-5} M) for L were prepared by using a universal buffer solution. The absorption of these solutions was recorded (using the pH value as a reference closure) with a difference of wavelengths of 330-530 nm.

3. DISCUSSION AND RESULTS

The azo dye L is stable in air and all solvents that used, with their properties in Table 1.

Table 1. Properties of azo dye L

Molecular Formula	Molecular Weight ($g.mol^{-1}$)	Color	M.P. ℃	λ_{max} nm	Yield %
$C_{21}H_{28}N_4O_5$	416.5	Orange	208-211	430	85

3.1 Identification of the prepared azo dye L

3.1.1 FT- IR spectra of azo dye L

Infrared radiation is one of the most common methods for examining ligands and knowing the absorption bands of effective groups within the internal structure of the molecule and its usefulness in following up the occurrence of the interaction through the disappearance of bands and the emergence of new bands. The most important absorptions visible in the infrared technology of the compound azo dye L in the chemical compound (Figure 1) are presented in Table 2. The observed major bands are the sharp band (1600 cm^{-1}) due to ν (C=C) and the band at 1454 cm^{-1} due to the group ν (N=N).

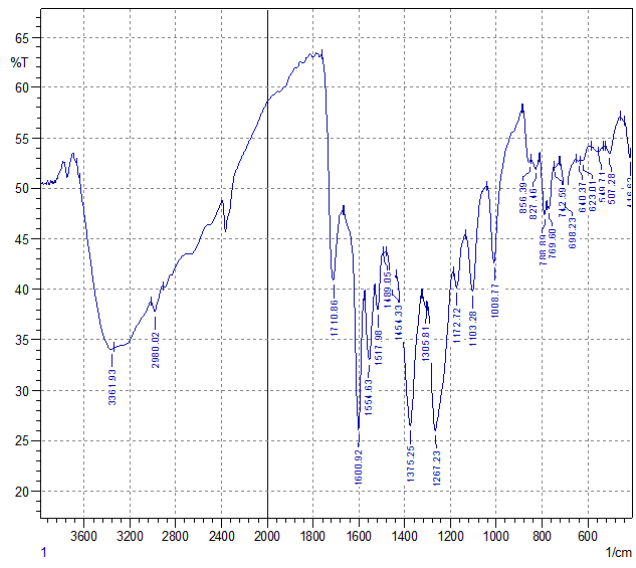

Figure 1. The FT-IR spectrum of azo dye L

3.1.2 Mass spectrum of azo dye L

Mass spectrometry is one of the most important techniques used in determining the molecular formula of newly prepared

chemical compounds, as well as studying their dissociation pathways. Depending on this technique, the mass spectrometry of the prepared azo dye has been studied. The mass spectrum of the prepared azo dye L (Figure 2) indicates the appearance of the molecular ion peak at 416 m/z, and the spectrum indicates the appearance of the base ion peak at 43m/z.

Table 2. Infrared FT-IR data for the azo dye L was prepared in the lab

V(OH) cm^{-1}	V(C-H)$_{Ar}$ cm^{-1}	V(C=O) cm^{-1}	V(N=N) cm^{-1}	V(C=C) cm^{-1}	V(C-N) cm^{-1}
3361 br	2980 m	1710 m	1454 w	1600 s	1375 s
br = brood, w = weak, s = strong, m = medium					

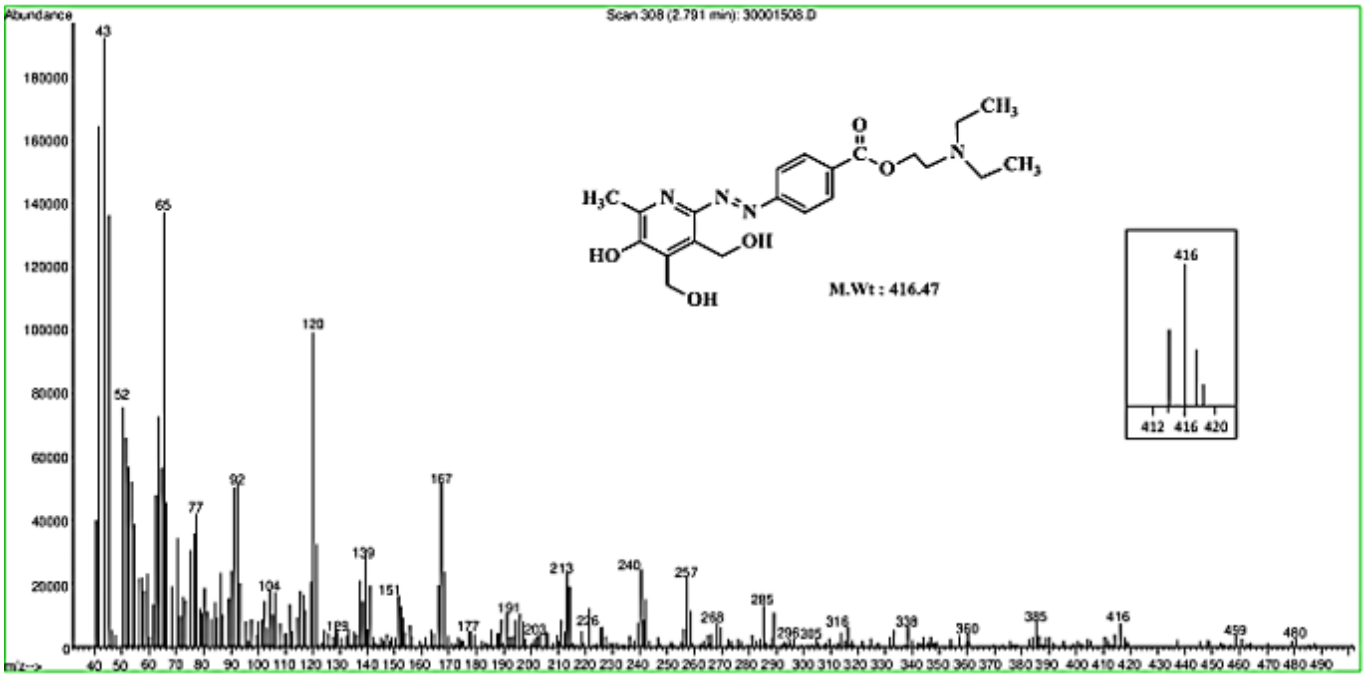

Figure 2. The mass spectrum of azo dye L

3.2 Effect of solvents on the visible absorption spectra of the prepared dye L

We conclude from this study that there are changes in the location and intensity of the electron absorption peaks. The interactions between the solvent and the solute are classified into two types. First, specific interaction results in the bonding of the solute molecules with the solvent molecules through hydrogen bonds and the formation of charge transfer complexes. Second: Specific interaction of this type results in electrostatic attraction between the solute and the solvent due to the effect of the dipole-dipole moment and the induced dipole-dipole effect, as well as the dispersion force. Figure 3 displays the spectra of azo dye L in many solvents of distinct polarities (n-hexane, benzene, 1,4-dioxane, diethyl ether, chloroform, ethyl acetate, THF, dichloromethane, cyclohexanol, acetone, ethanol, and DMSO). The dye L hazing two connects at all solvents relied on at 360 nm. And at a range of 470-490 nm. The levels of fluids were shifted from less absorbance (n-hexane, which is considered a non-polar solvent, to the highest one, DMSO). The absorption spectra of different polar solvents are affected by the solubility of the solvent or by the dielectric effects (Table 3).

The function for dielectric plot [(D-1)/(D+1)] in opposition to the λmax of azo dye (L) (Figure 4), where we note that it gives a high linear relationship with solvents of moderate polarity. A linear relationship, indicating that the dielectric constant is the most important factor affecting solvation.

Table 3. The effect of dielectric constant function of solvents on the max. wavelength of dye

Solvent	Sym.	(D-1) /(D+1)	λ_{max1} nm	$\varepsilon_{max} \times 10^4$ l.mol^{-1}.cm^{-1}	λ_{max2} nm	$\varepsilon_{max} \times 10^4$ l.mol^{-1}.cm^{-1}
n-Hexane	1	0.308	360	0. 964	480	0.365
benzene	2	0.390	360	1.109	480	1.549
1,4-Dioxane	3	0.394	360	1.111	480	1.800
Diethyl ether	4	0.625	360	1.595	470	1.020
Chloroform	5	0.655	360	0.895	480	1.576
Ethyl acetate	6	0.730	360	1.339	470	1.382
THF	7	0.767	360	1.454	480	1.227
DCM	8	0.802	360	0.874	480	1.954
Cyclohexanol	9	0.861	360	0.938	480	1.285
Acetone	10	0.907	360	1.143	470	1.528
Ethanol	11	0.920	360	1.783	480	0.556
DMSO	12	0.958	360	1.264	490	1.201

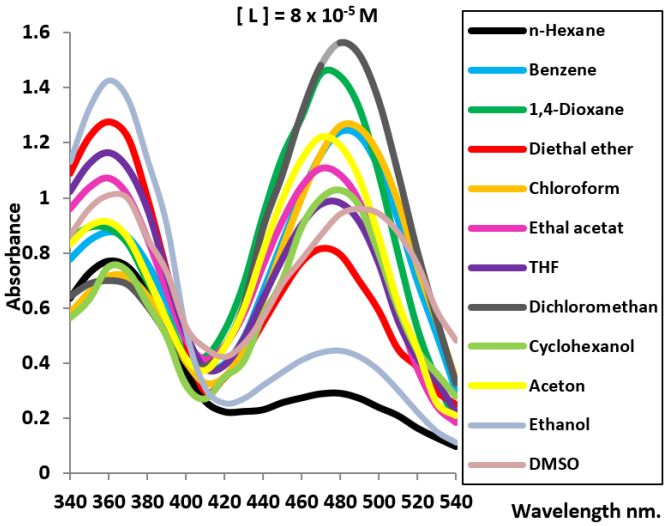

Figure 3. The electronic spectra of azo dye L at different solvents

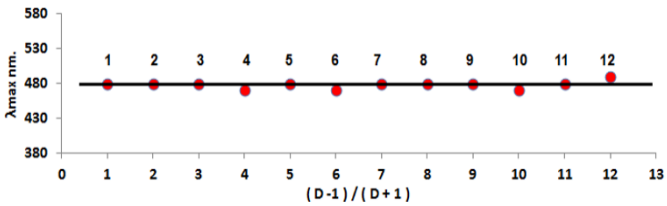

Figure 4. The relation of dielectric constant function of solvents on the max wavelength of azo dye L

3.3 Acid – Base properties of the azo dye L

From Figure 5, it was shown that the spectra of azo dye L at different pH values had two highest absorbance bands: the first at pH 4 at pH range (2-8) at wavelength (380 nm) and the second at pH 12 at pH range (9-12) at wavelength (430 nm). All spectra show one band except for at acidic medium pH 2 and 3 values at 380 and 480 nm, respectively. Study of the effect of the acid function and its benefit: A very important application is to know the ionization and protonation constants. These conditions or constants may help us in finding the acid function for this dye to work as a corrosion inhibitor. The spectra show two isopiestic points at 385 and 400 nm. There is another isopiestic point below 330 nm that was not seen in the spectra.

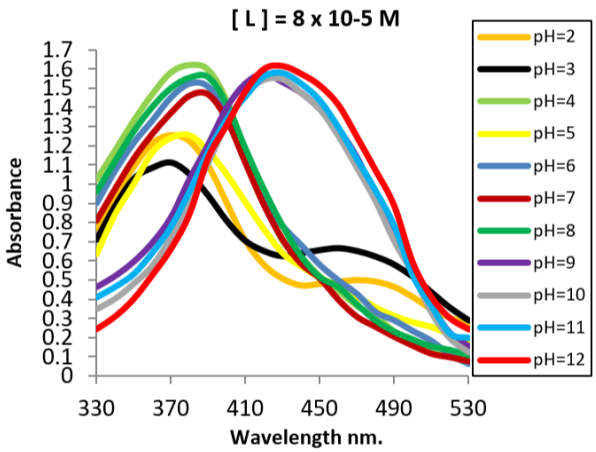

Figure 5. The electronic spectra of azo dye L at different pH values

Table 4. The half-height method parameters for calculation of protonation and ionization constants of azo dye L

A_{min}	A_1	$A_{1/2}$	pK_{p1}	pK_{p2}	pK_a
0.50	0.70	0.60	2.78	------	------
0.63	0.78	0.71	------	5.50	------
0.70	1.58	1.14	------	------	8.50

From the absorbance–pH curves of the azo dye, L was plotted to determine the ionization and protonation constants at certain wavelengths (430 nm) (Figure 6). By the aid of the half-height method, the pK values were obtained by this relation.

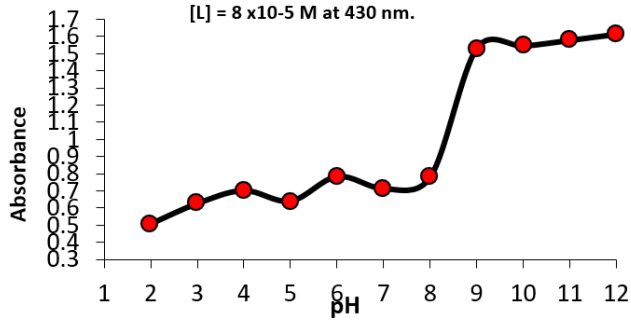

Figure 6. The relation between the absorbance of azo dye L and different pH values

Then the protonation (pK_p) and ionization (pK_a) constants (Table 4), were measured using the absorbance – pH curve (Figure 6).

Where pK_a is ionization constant of phenolic group of pyridine ring, pK_{p1} is the protonation constant of aliphatic nitrogen of procaine molecule and pK_{p2} is the constant of nitrogen atom of pyridine ring. The mechanism of the purification and ionization processes of the pure azo dye L was suggested as shown in Scheme 2.

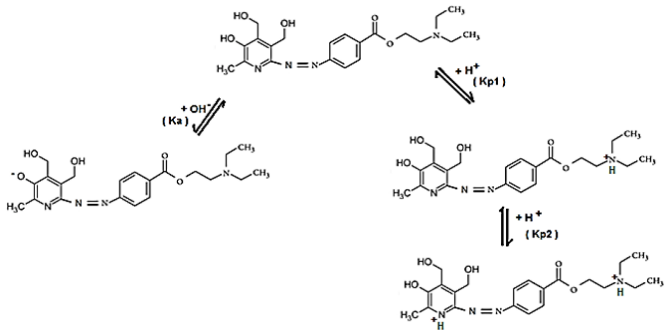

Scheme 2. Suggested mechanism of protonation and ionization of azo dye L

3.4 Kinds of buffer solution of pH 12

To alright the impact of kind of buffer solutions to get the highest absorbance of azo dye L (pH 12), several buffer solutions were prepared that give pH 12 (1 = Universal, 2 = Hexamine, 3 = [H_3BO_3+NaOH]+NaOH, 4 = KCl + NaOH, 5 = $Na_2HPO_4.2H_2O$+NaOH). It was discovered from Figure 7. A sincere kind of buffer solution of pH 12 is hexamine.

3.5 Computational chemistry calculations

Quantum chemistry calculations have proven to be an

effective tool for studying the corrosion inhibition mechanism [19-21] if quantum chemistry calculation methods are used to obtain information that can be obtained from experimental data [22], and one of the most important prominent molecular properties obtained through computational chemistry calculations, which are summarized in Table 5, the most important of which are (Higher Occupant Molecular Orbital Energy (EHOMO), Lower Occupant Molecular Orbital Energy (ELUMO), Electronegativity, Chemical hardness, Softness, Number of transferred electrons (ΔN), Ionization potential and Dipole moment, as for the forms of engineering alignments (optimized geometrical. The stereoforms of (HOMO) and (LUMO) and the surface electrostatic potential (ESP) of the pre-prepared L1 inhibitor molecules [23] and the new derived damper L2 are shown in Table 5.

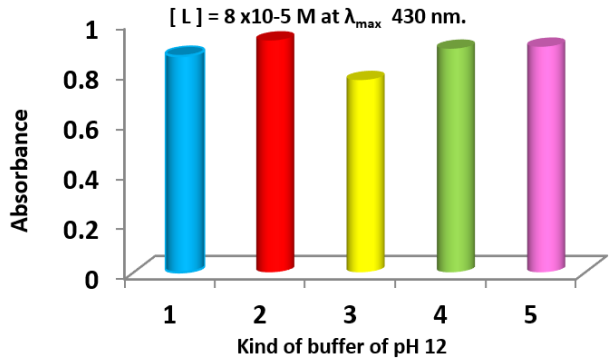

Figure 7. Kinds of buffer solutions of pH 12 at λmax (430 nm.)

Table 5. Quantitative chemical data values of the inhibitors studied measured using the density functional theory method, B3LYP level, basis set elements 6-31G+(d) and Gaussian09

Quantum Chemical Parameters	L1	L2
Total Energy (kJ.mol^{-1})	-3149461.6698	-3459125.0320
Dipole Moment (Debyes)	4.1992	4.2049
E_{HOMO} *(eV)*	-5.8818	-5.9637
E_{LUMO} *(eV)*	-2.333	-2.337
$\Delta E_{gab} = E_{LUMO} - E_{HOMO}$ *(eV)*	3.5487	3.6262
Ionization Potential, $I = -E_{HOMO}$	5.8818	5.9637
Electron Affinity, $A = -E_{LUMO}$	2.33312	2.33747
Electronegativity (χ), $-\frac{1}{2}(E_{HOMO} + E_{LUMO})$	4.1075	4.1506
Chemical Hardness (η), $\Delta E_{gab}/2$	1.7743	1.8131
Softness (σ), $1/\eta$	0.5636	0.5515
Chemical Potential $\mu = -1/2(I + A)$	-4.107	-4.151
Number of Transferred Electrons $\Delta N = \chi_{Fe} - \chi_{inh} / [2(\eta_{Fe} + \eta_{inh})]$	0.81511	0.78578

3.5.1 HOMO & LOMO

It can be seen that the highest occupied molecular orbitals (HOMO) and the lowest unoccupied molecular orbitals (LUMO) are widely distributed on both sides of the two azo dyes studied, which indicates that the N=N group in the pre-prepared azo dye L1 and the new azo dye derived from it, L2. It can be seen that the highest occupied molecular orbitals (HOMO) and the lowest unoccupied molecular orbitals (LUMO) are widely distributed on both sides of the two azo dyes studied, which indicates that the (N=N) group in the pre-prepared azo dye (L1) and the new azo dye derived from it (L2). And other groups as groups (OH), which are considered as electron donor centers and other electron receptors, respectively, and both types act as main adsorption centers. The incorporation of the damper on the exterior of the steel occurs on the basis of donor-acceptor reactions between the lone pairs on the (N and O) atoms in the structure of the two azo dyes (L1 and L2) and the vacant orbitals of the iron atom in which the boundary orbitals (HOMO and LUMO) of chemical species play a vital role in determining their absorption and interaction. The higher the energy value of the highest occupied molecular orbital (EHOMO), the greater its tendency to donate electrons to the appropriate receiving molecules with empty low-energy molecular orbitals and thus increase the inhibition efficiency, as well as the lower the energy of the lowest unoccupied molecular orbital (ELUMO), which makes the prepared azo dye molecule receive electrons, also increases the inhibition efficiency [24, 25]. Among the molecules of the studied azo dyes, the L1 molecule has the highest energy value of the highest occupied molecular orbital (EHOMO) (-5.88 eV) in contrast to the L2 molecule structure, which has an energy (EHOMO) of (-5.96 eV), so the L1 molecule is an easy donor of electrons, which enhances its effectiveness on inhibition.

3.5.2 Energy gap (ΔEgab)

The value of the so-called energy gap (ΔEgab), which represents the difference between EHOMO and ELUMO, can be linked to the two inhibitors studied according to the frontier molecular orbital theory (F.M.O.) of the chemical reaction. The smaller the orbital energy gap (ΔEgab), the stronger the inhibitory reaction on the steel appears, and thus an improvement in the efficiency of the retarding, as ΔEgab showed values of 3.5487 and 3.6262 for both L1 and L2, respectively [26, 27]. According to the theory of hard and soft acids and bases (HSAB), solid acids tend to react with hard bases, and soft acids react with soft bases. According to this theory, which considers iron to be a soft acid, it tends to interact more with the molecule L1, which can be considered a soft base because it has a low hardness value of 1.813 eV and a high softness value of 0.5515 eV. Thus, the L1 damper shows a better inhibition efficiency compared to the L2 damper with a hardness value of 1.7743 eV and a softness value of 0.5636 eV [28].

3.5.3 ESP

The study of the ESP and the electrostatic potential map of the inhibitor molecule (L1) compared to (L2), shown in Figures 8 and 9, is very useful to detect the locations of electron density on specific atoms. Therefore, its importance can be included in determining the positive, negative, and neutral electrostatic potentials of all atoms of the studied molecule so that we can determine the locations of electrostatic attack that prefer the high negative region

(regions of increased electron density), which are red in color, while the high positive regions (regions of low electron density), which are blue in color, are the preferred locations for nuclear attack [29], respectively. The study of ESP and electrostatic potential map of inhibitor molecules (L1 and L2) shown in Table 5 are very useful for detecting electron density locations that lie on specific atoms. Thus, it's crucial to include it in the determination of the positive, negative, and neutral electrostatic potential of all atoms of the studied molecule in order to determine which electrolytic attack sites favor the high negative region (areas of electron density increase), which are red in color, while high positive regions (electron density deficiency zones) that are blue are preferred sites for nucleophile attack [26]. Therefore, it is assumed from the above that the experimental results, if conducted, must have a corrosion refusal efficiency of the inhibitor (L2) elevated than the value of the inhibitor inhibition efficiency (L1) according to the theoretical results in computational chemistry.

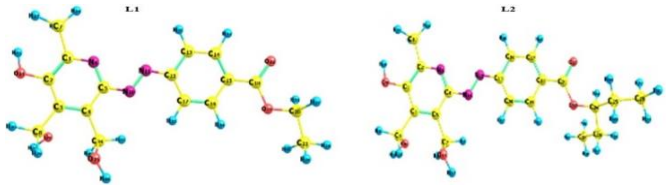

Figure 8. Optimized geometry of L1 and L2

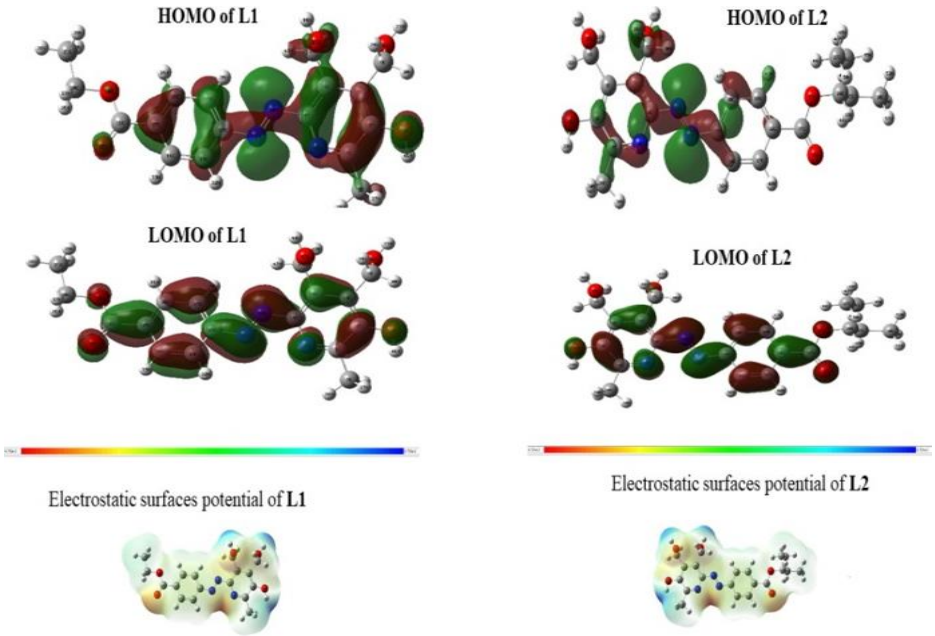

Figure 9. HOMO, LOMO, and Electrostatic surfaces potential of L1 and L2

3.5.4 The number of electrons transferred (ΔN)

The value of the quantity of moved electrons (ΔN) indicates the ability of the inhibitor molecule to give electrons; the higher the value of (ΔN), the better the ability of the studied inhibitory molecule for electron donation of receptive species characterized by electron deficiency (represented in this study by orbitals d iron metal surface atoms). In the field of corrosion inhibitors, high values of the number of electrons transferred (ΔN) mean that there is a high tendency for the reaction of the inhibitor molecule studied on the metal surface throughout adsorption processes, indicating increased inhibition efficiency. According to Lukovit's et al. [30], it was hypothesized that the higher the value of the number of electrons transferred (ΔN), the greater the electron donation ability of the studied inhibitor molecule of the orbitals of the metal surface atoms, which leads to a boost in the prohibition efficiency, provided that the value of the number of electrons transferred (ΔN) is 3.6 [26, 30, 31]. ΔN was calculated according to Pearson's theorem using the equation [$\Delta N = \chi Fe - \chi inh /[2(\eta Fe + \eta inh)]$ [32, 33]. χFe and χinh represent the electronegativity of iron metal and the damper, respectively, while ηFe and ηinh represent the chemical hardness of iron metal and the damper, respectively. The theoretical values for χFe and ηFe are 7.0 and 0 eV mol^{-1}, respectively, while the values of the number of electrons transferred (ΔN) for both azo dyes (L1 and L2) were 0.7858 and 0.8151.

4. CONCLUSIONS

The results of experimental showed that L2 have a corrosion refusal efficiency of the inhibitor more than the value of the inhibitor inhibition efficiency L1, and based on the theoretical results in computational chemistry. It can also be an anti-corrosion agent and an alternative to anti-corrosion materials, as they are expensive.

CONTRIBUTION STATEMENT

HAA and IAA were contributed in designing, analysis, and writing the manuscript; HTO, GAM, and NAMO were contributed in the experiments of synthesis and analysis. All authors were approved the final version of manuscript.

REFERENCES

[1] Abdalla, N.A., El-Haty, M.T., Adam, F.A.E., Hassan, F.W. (2013). Complexes of Cu (II), Co (II), Ni (II), Zn (II), Zr (IV), Ce (III), La (III) AND UO2 (II) with arylazo pyriimidine derivatives. Revue Roumaine de Chimie, 58(11-12): 899-913.

[2] Almeida, M.R., Stephani, R., Santos, D., de Oliveira,

L.F.C. (2010). Spectroscopic and theoretical study of the 'Azo'-Dye e124 in condensate phase: Evidence of a dominant hydrazo form. The Journal of Physical Chemistry A, 114(1): 526-534. https://doi.org/10.1021/jp907473d

[3] Al-Waeli, J.H., AbdullMajed, H.A., Ismael, S.M. (2024). Studies of spectroanalytical and the biological effectiveness of the Azo compound (J25) prepared from Ethyl p-aminobenzoate. Journal of Basrah Researches (Sciences), 50(1). https://doi.org/10.56714/bjrs.50.1.15

[4] Senol, D., Kaya, I. (2015). Synthesis and characterization of novel polyamines containing different substitute groups via chemical oxidative polymerization. Journal of the Chinese Chemical Society, 62(5): 429-438. https://doi.org/10.1002/jccs.201400525

[5] Patil, C.J., Nehete, C.A. (2015). The azo derivatives of salicylic acid. International Journal of Pharmaceutical Sciences Review and Research, 33(2): 248-256.

[6] Benkhaya, S., M'rabet, S., El Harfi, A. (2020). Classifications, properties, recent synthesis and applications of azo dyes. Heliyon, 6(1): e03271. https://doi.org/10.1016/j.heliyon.2020.e03271

[7] Gaber, M., Ayad, M.M., El-Sayed, Y.S.Y. (2005). Synthesis, spectral and thermal studies of Co (II), Ni (II) and Cu (II) complexes 1-(4, 6-dimethyl-pyrimidin-2-ylazo)-naphthalen-2-ol. Spectrochimica Acta Part A: Molecular and Biomolecular Spectroscopy, 62(1-3): 694-702. https://doi.org/10.1016/j.saa.2005.02.039

[8] Yin, J., Yu, G.A., Guan, J., Mei, F., Liu, S.H. (2005). Synthesis and properties of conjugated bimetallic ruthenium complexes with σ, σ-bridging azobenzene chains. Journal of Organometallic Chemistry, 690(19): 4265-4271. https://doi.org/10.1016/j.jorganchem.2005.06.031

[9] Tomai, P., Dal Bosco, C., D'Orazio, G., Scuto, F.R., Felli, N., Gentili, A. (2022). Supercritical fluid chromatography for vitamin and carotenoid analysis: An update covering 2011-2021. Journal of Chromatography Open, 2: 100027. https://doi.org/10.1016/j.jcoa.2021.100027

[10] Saleem, M.S., Mohammed, Z.A. (2013). A spectrophotometric micro determination of pyridoxine hydrochloride by coupling diazometry. Journal of Education and Science, 26(5): 23-35. https://doi.org/10.33899/edusj.2013.163052

[11] Kadir, A.A. (2010). Spectrophotometric determination of vitamin B6 by coupling with diazotized p-nitroaniline. Al-Rafidain Journal of Medical Sciences, 21: 49-59. https://doi.org/10.33899/rjs.2010.36845

[12] Ali, H., Majeed, H.A.S.A., Al-Asadi, I., Abdulredha, A., Hussain, A. (2018). Structures effect of two azo dyes associated with their antimicrobial activity. Journal of Chemical, Biological and Physical Sciences, 8: 171-185. https://doi.org/10.24214/jcbps.A.8.2.17185

[13] Al AlBaheley, N., Fahad, T.A., Ali, A.A. (2021). Synthesis, spectroscopic, and thermal studies of azo compounds from luminol and procaine with acetylacetone and their complexes. Journal of Physics: Conference Series, Basrah, Iraq, 2063(1): 012016. https://doi.org/10.1088/1742-6596/2063/1/012016

[14] Fahad, T.A., Yaqoob, R.H., Ali, A.A. (2017). Antimicrobial activity studies, preparation and characterization of new azo complexes driven from n-(4-hydroxyphenyl) acetamide. World Journal of Pharmaceutical Research, 6(5): 101-111. https://doi.org/10.20959/wjpr20175-8385

[15] Ali, N.W., Ali, A.A. (2016). Preperation and spectroanalytical studies of two new azodyes derived from procaine hydrochloride and metaclopramide. World Journal of Pharmaceutical Research, 5(10): 127-140. https://doi.org/10.20959/wjpr201610-7133

[16] Thuiny, H.T., Fahad, T.A., Ali, A.A. (2021). Preparation, analytical studies and application of a new azodye derived from pharmaceutical materials (Procaine Hydrochloride & Salicylic acid). In Journal of Physics: Conference Series, Basrah, Iraq, 2063(1): 012024. https://doi.org/10.1088/1742-6596/2063/1/012024

[17] Al-Muhsin, A.A., Fahad, T.A., Ali, A.A. (2021). Preparation and characterization azo dyes derived from 4-hydroxycoumarin and studying their analytical Applications. In Journal of Physics: Conference Series, Diwaniyah, Iraq, 1999(1): 012010. https://doi.org/10.1088/1742-6596/1999/1/012010

[18] Dean, J.A. (1999). Lange's Handbook of Chemistry.

[19] Bentiss, F., Lebrini, M., Lagrenée, M. (2005). Thermodynamic characterization of metal dissolution and inhibitor adsorption processes in mild steel/2, 5-bis (n-thienyl)-1, 3, 4-thiadiazoles/hydrochloric acid system. Corrosion Science, 47(12): 2915-2931. https://doi.org/10.1016/j.corsci.2005.05.034

[20] Xiao-Ci, Y., Hong, Z., Ming-Dao, L., Hong-Xuan, R., Lu-An, Y. (2000). Quantum chemical study of the inhibition properties of pyridine and its derivatives at an aluminum surface. Corrosion Science, 42(4): 645-653. https://doi.org/10.1016/S0010-938X(99)00091-8

[21] Zhao, P., Liang, Q., Li, Y. (2005). Electrochemical, SEM/EDS and quantum chemical study of phthalocyanines as corrosion inhibitors for mild steel in 1 mol/l HCl. Applied Surface Science, 252(5): 1596-1607. https://doi.org/10.1016/j.apsusc.2005.02.121

[22] Kabanda, M.M., Murulana, L.C., Ozcan, M., Karadag, F., Dehri, I., Obot, I.B., Ebenso, E.E. (2012). Quantum chemical studies on the corrosion inhibition of mild steel by some triazoles and benzimidazole derivatives in acidic medium. International Journal of Electrochemical Science, 7(6): 5035-5056. https://doi.org/10.1016/S1452-3981(23)19602-7

[23] Chaitra, T.K., Mohana, K.N., Tandon, H.C. (2016). Study of new thiazole based pyridine derivatives as potential corrosion inhibitors for mild steel: Theoretical and experimental approach. International Journal of Corrosion, 2016(1): 9532809. https://doi.org/10.1155/2016/9532809

[24] Li, W.H., Zhao, X., Liu, F.Q., Deng, J.Y., Hou, B.R. (2009). Investigation on the corrosion inhibitive effect of 2H—pyrazole—triazole derivatives in acidic solution. Materials and Corrosion, 60(4): 287-293. https://doi.org/10.1002/maco.200805081

[25] Obaid, H.T., Kadhum, M.Y., Abdulnabi, A.S. (2022). Azo Schiff base derived from 2-hydroxy-1-naphthaldehyde as corrosion inhibitors for carbon steel in HCl medium: Experimental and theoretical studies. Materials Today: Proceedings, 60: 1394-1401. https://doi.org/10.1016/j.matpr.2021.10.380

[26] Meften, M.J., Radhi, W.A., Abulhail, A.N. (2018). Molecular structure and electronic characteristics study of imidazole and dioxol derivatives as corrosion inhibitors. A quantum methodology investigation.

Basrah Journal of Science, 36(C): 1-29. https://doi.org/10.29072/basjs.2018302
[27] Xia, S.W., Qiu, M., Yu, L.M., Liu, F.G., Zhao, H.Z. (2008). Molecular dynamics and density functional theory study on relationship between structure of imidazoline derivatives and inhibition performance. Corrosion Science, 50(7): 2021-2029. https://doi.org/10.1016/j.corsci.2008.04.021
[28] Chaitra, T.K., Mohana, K.N., Gurudatt, D.M., Tandon, H.C. (2016). Inhibition activity of new thiazole hydrazones towards mild steel corrosion in acid media by thermodynamic, electrochemical and quantum chemical methods. Journal of the Taiwan Institute of Chemical Engineers, 67: 521-531. https://doi.org/10.1016/j.jtice.2016.08.013
[29] Aksh, A.K., Nabi, A.S.A., Obaid, H.T. (2024). Peganum harmala extract as an eco-friendly corrosion inhibitor for carbon steel N80 in 1 M HCl: Electrochemical and surface morphological studies. Nanotechnol Perceptions, 20(S3): 33-49. https://doi.org/10.62441/nano-ntp.v20iS3.571
[30] Lukovts, I., Kalman, E., Zucchi, F. (2001). Corrosion inhibitors—Correlation between electronic structure and efficiency. Corrosion, 57(1): 3-8. https://doi.org/10.5006/1.3290328
[31] Dhaef, H.K., Al-Asadi, R.H., Shenta, A.A., Mohammed, M.K. (2021). Novel bis maleimide derivatives containing azo group: Synthesis, corrosion inhibition, and theoretical study. Indonesian Journal of Chemistry, 21(5): 1212-1220. https://doi.org/10.22146/ijc.64614
[32] Pearson, R.G. (1988). Absolute electronegativity and hardness: Application to inorganic chemistry. Inorganic Chemistry, 27(4): 734-740. https://doi.org/10.1021/ic00277a030
[33] Obaid, H.T., Mutar, M.M., Ali, S.H. (2025). Sulfasalazine as a corrosion inhibitor on carbon steel metal surfaces in acidic media using the hydrogen evolution method: Experimental and theoretical studies. Indonesian Journal of Chemistry, 25(1): 90-99. https://doi.org/10.22146/ijc.95852